[CANCER RESEARCH 64, 7936–7946, November 1, 2004]

Luteolin Inhibits Vascular Endothelial Growth Factor-Induced Angiogenesis; Inhibition of Endothelial Cell Survival and Proliferation by Targeting Phosphatidylinositol 3′-Kinase Activity

Eleni Bagli,[1] Maria Stefaniotou,[2] Lucia Morbidelli,[3] Marina Ziche,[3] Konstantinos Psillas,[2] Carol Murphy,[4] and Theodore Fotsis[1,4]

[1]Laboratory of Biological Chemistry and [2]Department of Ophthalmology, Medical School, University of Ioannina, Ioannina, Greece; [3]Department of Molecular Biology, University of Siena, Siena, Italy; and [4]Foundation of Research and Technology-Hellas, Biomedical Research Institute, Ioannina, Greece

ABSTRACT

In an attempt to identify phytochemicals contributing to the well-documented preventive effect of plant-based diets on cancer incidence and mortality, we have previously shown that certain flavonoids inhibit *in vitro* angiogenesis. Here, we show that the flavonoid luteolin inhibited tumor growth and angiogenesis in a murine xenograft model. Furthermore, luteolin inhibited vascular endothelial growth factor (VEGF)-induced *in vivo* angiogenesis in the rabbit corneal assay. In agreement, luteolin inhibited both VEGF-induced survival and proliferation of human umbilical vein endothelial cells (HUVECs) with an IC_{50} of about 5 μmol/L. Luteolin inhibited VEGF-induced phosphatidylinositol 3′-kinase (PI3K) activity in HUVECs, and this inhibition was critical for both the antisurvival and antimitotic affects of the compound. Indeed, luteolin abolished VEGF-induced activation of Akt, a downstream target of PI3K conveying both survival and mitotic downstream signals. Because overexpression of a constitutively active form of Akt rescued HUVECs only from the antisurvival effects of luteolin, the result indicated that luteolin targeted mainly the survival signals of the PI3K/Akt pathway. With regard to its antimitotic activity, luteolin inhibited VEGF-induced phosphorylation of p70 S6 kinase (S6K), a downstream effector of PI3K responsible for G_1 progression. Indeed, VEGF-induced proliferation of HUVECs was sensitive to rapamycin, an inhibitor of p70 S6K activation. Surprisingly, luteolin did not affect VEGF-induced phosphorylation of extracellular signal-regulated kinase 1/2 mitogen-activated protein kinases, a pathway that is considered important for the mitotic effects of VEGF. Thus, blockade of PI3K by luteolin was responsible for the inhibitory effects of the compound on VEGF-induced survival and proliferation of HUVECs. The antisurvival effects of luteolin were mediated via blockage of PI3K/Akt-dependent pathways, whereas inhibition of the PI3K/p70 S6K pathway mediated the antimitotic effects of the compound.

INTRODUCTION

Angiogenesis, the formation of new vessels from preexisting ones, is a strictly regulated and self-restricted physiological process. A growing number of diseases, including rheumatic arthritis, psoriasis, and diabetic retinopathy, derive from excessive, deregulated angiogenesis. However, the most important manifestation of pathological angiogenesis is that seen in the vicinity of solid tumors. Indeed, well-vascularized tumors expand both locally and by metastasis, whereas avascular tumors do not grow beyond a diameter of 1 to 2 mm (1).

One of the most important factors regulating angiogenesis is vascular endothelial growth factor (VEGF). Indeed, VEGF regulates key angiogenic responses of endothelial cells (ECs), for instance proliferation, migration, and differentiation, as well as protection from apoptosis (2). In cancer, VEGF is overexpressed after hypoxia (3, 4) and/or as a consequence of the genetic changes of cancer, such as mutations of oncogenes and tumor suppressor genes (5). Indeed, most tumors express high levels of VEGF, whereas the adjacent ECs express VEGF receptors 1 and 2 (6), establishing an angiogenic loop. Thus, in a wide range of cancers, VEGF levels in plasma or in biopsy specimens have critical prognostic importance for the outcome of tumor growth and influence the therapy used (7). The importance of VEGF in the stimulation of tumor angiogenesis is obvious from the fact that it represents one of the main targets for antiangiogenic anticancer drug development. Hence, many methods have been developed for inhibiting VEGF activity. These drugs involve the use of anti-VEGF antibodies, soluble receptors, peptides that interfere with VEGF binding, and molecules that interfere with VEGF signaling (5, 7). Indeed, antiangiogenic gene therapy of cancer with adenoviruses expressing soluble VEGFRs in mice gave superior results compared with other modes of antiangiogenic treatment (8).

VEGF is found in many isoforms (VEGF-A, -B, -C, -D, and -E) that derive from the alternative splicing of the same gene (2). These isoforms transduce their signals to the nucleus mainly through three receptors, VEGFR-1, -2, and -3 (9). Of these receptors, VEGFR-2 appears to play a critical role in the regulation of angiogenesis (9), whereas VEGFR-1 also seems to participate in pathological angiogenesis (10); VEGFR-3 is responsible for lymphangiogenesis (11). VEGFR-2 receptor has tyrosine kinase activity and phosphorylates secondary messengers, which appear to regulate EC proliferation via activation of extracellular signal-regulated kinase (ERK) 1/2 mitogen-activated protein kinases (MAPKs; ref. 12) and p70 S6 kinase (S6K; ref. 13), migration of ECs via the stress-activated protein kinase 2/p38 pathway (14), and survival of ECs via Akt activation (15).

Dietary factors contribute to about a third of potentially preventable cancers (16), and the long-known preventive effect of plant-based diets on tumorigenesis and other chronic diseases is well documented (17). These data indicate that certain plant-derived dietary groups might contain phytochemicals that exert antimitotic and antitumorigenic effects, thereby offering anticancer protection to individuals consuming such diets. In previous studies, we have examined this possibility by screening urine of human subjects consuming a diet rich in plant products for the presence of antimitotic and antiangiogenic compounds. This work led to the identification of the isoflavonoid genistein as well as a number of the isomeric flavonoids, such as luteolin, as potent inhibitors of tumor cell proliferation and *in vitro* angiogenesis (18, 19). Flavonoids are widely distributed in the plant kingdom, rendering them a very attractive target for additional studies. In the present study, we have addressed the effect of luteolin on VEGF-induced angiogenesis using the rabbit corneal micropocket assay and on tumor growth and angiogenesis using a murine xenograft

Received 10/2/03; revised 8/20/04; accepted 9/7/04.

Grant support: Work at the University of Ioannina was supported by a research grant from the European Commission Contract No. QLRT-2000-00266 (PHYTOPREVENT). Work at the University of Siena was partially funded by a Research Grant from the European Commission Contract No. QLRT-1999-00505 (POLYBIND) and the European Nutrigenomics Organization.

The costs of publication of this article were defrayed in part by the payment of page charges. This article must therefore be hereby marked *advertisement* in accordance with 18 U.S.C. Section 1734 solely to indicate this fact.

Requests for reprints: Theodore Fotsis, Laboratory of Biological Chemistry, Medical School, University of Ioannina, 45110 Ioannina, Greece. Phone: 30-26510-97560; Fax: 30-26510-97868; E-mail: thfotsis@cc.uoi.gr.

model. Moreover, we have investigated the effect of luteolin on several signaling pathways emanating from VEGFR-2.

MATERIALS AND METHODS

Antibodies and Recombinant Proteins. Human $VEGF_{165}$ was purchased from R&D Systems, Inc (Minneapolis, MN). Luteolin was obtained from Sigma (St. Louis, MO) and diluted in dimethyl sulfoxide (DMSO)/EtOH, (1:1) by volume. The polyclonal antibodies anti–phospho-Akt (Ser^{473}), anti-Akt, anti–phospho-MAPK, anti-MAPK, anti–phospho-p38, and anti-p38 were from Cell Signaling Technology, Inc. (Beverley, MA). The mouse monoclonal anti–phospho-tyrosine antibody (P3300) was obtained from Sigma. The rabbit polyclonal anti–FLK-1 antibody (C-1158) and the goat antiactin antibody (SC-1616) were purchased from Santa Cruz Biotechnology (Santa Cruz, CA). The rabbit polyclonal anti-PI3K antibody (p85; 06-195) was purchased from Upstate Biotechnology (Lake Placid, NY). The Ki67 antibody was a gift from Mary Bai (University of Ioannina, Ioannina, Greece), anti–phospho-p70 S6K (Thr^{389}) antibody was a gift from A. Papapetropoulos (University of Patras, Patras, Greece), and rapamycin was a gift from I. Lazaridis (University of Ioannina). The 12Ca5 [anti-hemagglutinin (HA)] monoclonal antibody was purified from the corresponding hybridoma using standard techniques. All secondary antibodies were purchased from Dianova GmbH (Hamburg, Germany). The anti-extradomain B (ED-B) antibody was kindly provided by Philogen S.p.A. Monteriggioni-Siena (Italy).

Cell Culture. Human umbilical vein ECs (HUVECs) were plated on dishes precoated with rat collagen type I (Becton Dickinson Biosciences, San Jose, CA) and cultured in M199 medium supplemented with 20% fetal calf serum (FCS), EC growth supplement (Sigma), heparin (Sigma), and penicillin-streptomycin. All media and sera for cell culture were purchased from Invitrogen (Carlsbad, CA) and were endotoxin-free. Cells were split 1:4 when they reached confluence, and passages between passage 4 and passage 10 were used for these experiments. A-431 cells were purchased from American Type Culture Collection (Rockville, MD) and cultured in Dulbecco's modified Eagle's medium supplemented with 4,500 g/L glucose and 10% FCS. All compounds and solvents added to the cells were tested for endotoxin content using the QCL1000 kit from BioWhittaker, Inc. (Walkersville, MD). Luteolin was resuspended in DMSO/EtOH (1:1 by volume) and added directly to the culture medium. Cells not receiving luteolin were incubated in the corresponding volume of DMSO/EtOH or left untreated. Rapamycin was resuspended in DMSO, and equivalent volumes of DMSO were used as solvent controls in all experiments.

Phosphatidylinositol 3′-Kinase Immunoprecipitation and Lipid Kinase Assay. Subconfluent cells were serum starved for 12 hours in medium containing 0.01% FCS and then incubated for 5 minutes with VEGF (30 ng/mL) in the presence or absence of luteolin. Cells were washed with ice-cold PBS containing 100 nmol/L vanadate and resuspended in ice-cold lysis buffer [1% Nonidet P-40, 50 mmol/L Tris (pH 7.5), and 150 mmol/L NaCl] supplemented with protease and phosphatase inhibitors. The lipid kinase activity of phosphatidylinositol 3′-kinase (PI3K) was measured according to previous reports (20), with minor modifications. Briefly, protein A-Sepharose beads (Sigma) containing immunoprecipitated PI3K from precleared lysates were washed twice with buffer A [20 mmol/L Tris (pH 7.4), 137 mmol/L NaCl, 1 mmol/L $MgCl_2$, and 1% Nonidet P-40], twice with 5 mmol/L LiCl in 0.1 mol/L Tris (pH 7.4), and twice with TNE [10 mmol/L Tris (pH 7.4), 150 mmol/L NaCl, 5 mmol/L EDTA, and 0.1 mmol/L Na_3VO_4]. All buffers were supplemented with protease and phosphatase inhibitors. The immunoprecipitates were then resuspended in TNE, and the PI3K activity was assayed using 0.2 mg/mL phosphatidylinositol 4,5-diphosphate (Sigma) as substrate in the presence of 58 μmol/L ATP, 10 μCi of [γ-^{32}P]ATP (5 mCi/mmol), and 14 mmol/L $MgCl_2$ for 10 minutes at 37°C. The reaction was stopped by the addition of 1 mol/L HCl and methanol:chloroform (1:1). After phase separation, the lipids in the organic phase were chromatographed using thin layer chromatography on oxalated silica gel 60 (Merck, Darmstadt, Germany). Chromatographed lipids were visualized by iodine staining and compared with the migration of known standards. An aliquot of each immunoprecipitated sample was analyzed by Western blot for p85 to confirm equal immunoprecipitated p85 in all samples.

Immunoprecipitation, Kinase Assay, and Evaluation of the Phosphorylation Status of VEGFR-2. Cells were serum starved for 24 hours in medium containing 5% FCS and stimulated with 30 ng/mL VEGF in the presence or absence of luteolin. Cells were washed with ice-cold PBS containing 100 nmol/L vanadate and suspended in cold lysis buffer [1% CHAPS, 10 mmol/L EDTA, 10% glycerol, 20 mmol/L Tris (pH 7.4), and 150 mmol/L NaCl, supplemented with protease and phosphatase inhibitors]. Kinase assay was carried out essentially as described previously (21). Briefly, protein A-Sepharose beads containing immunoprecipitated VEGFR-2 from precleared lysates were washed three times with lysis buffer, and the immune complex kinase assay was carried out in a total volume of 25 μL containing 50 mmol/L HEPES (pH 7.4), 10 mmol/L $MnCl_2$, 1 mmol/L dithiothreitol, and 5 μCi of [γ-^{32}P]ATP for 7 minutes at room temperature. The samples were analyzed by SDS-PAGE, and gels were incubated for 30 minutes in 2.5% glutaraldehyde and washed twice with 10% acetic acid/40% methanol. The gels were subsequently treated for 1 hour at 55°C in 1 mol/L KOH to remove serine-bound phosphates (22), washed with 10% acetic acid/40% methanol, stained with Coomassie Blue, dried, and exposed to film. An aliquot of each immunoprecipitated sample was analyzed by Western blot for VEGFR-2 to confirm equal immunoprecipitated VEGFR-2 in all samples.

To assess the tyrosine phosphorylation status of VEGFR-2, the immunoprecipitated receptor (as described above) was washed and resuspended in lysis buffer, subjected to SDS-PAGE, and blotted onto a nitrocellulose membrane. Tyrosine-phosphorylated residues were detected using a mouse anti–phospho-tyrosine antibody and an antimouse peroxidase-conjugated secondary antibody, followed by detection using a chemiluminescence-based system (Amersham Biosciences, Piscataway, NJ). The membranes were then stripped and reprobed with an anti–VEGFR-2 antibody to normalize the phosphorylation and expression of the receptor.

Evaluation of Akt, ERK1/2, p70 S6 Kinase, and p38 Phosphorylation. Cells were serum starved for 12 hours in medium containing 5% FCS and then treated with VEGF (50 ng/mL) in the presence or absence of either luteolin or rapamycin for 15 minutes. Cells were washed with ice-cold PBS and lysed in lysis buffer (1% SDS supplemented with protease and phosphatase inhibitors). The lysates were resuspended in Laemmli buffer, subjected to SDS-PAGE, and blotted onto a nitrocellulose membrane. Phosphorylated Akt, ERK1/2, p70 S6K, and p38 were detected using specific rabbit polyclonal antibodies and an antirabbit peroxidase-conjugated secondary antibody, followed by detection using a chemiluminescence-based system. The membranes were then stripped and reprobed with antibodies against Akt, ERK1/2, and p38 to normalize the phosphorylation data against expression of the kinases. In the case of p70 S6K, the membranes were reprobed with an antiactin antibody for normalization.

Recombinant Adenoviruses and Infection. Adenoviruses expressing either the HA-tagged constitutively active Akt [myristoylated-Akt (myrAkt)] or β-galactosidase were used. All viruses were amplified in 293 cells, and viral titers were estimated by plaque assay as described online.[5] For infection, HUVECs grown in 6-well plates were incubated with the recombinant adenoviruses at a multiplicity of infection of 25 for 2 hours. Then, the cells were washed and left for 30 hours in full medium until the experiment was carried out. The infection efficiency for all of the experiments was approximately 90%, as estimated by indirect immunofluorescence using the HA antibody (see method below). For β-galactosidase detection, cells were washed in PBS, fixed in 3.7% paraformaldehyde for 10 minutes at room temperature, and washed again in PBS. Cells were then incubated at 37°C until color development in a solution containing 5 mmol/L potassium ferricyanide, 5 mmol/L ferrocyanide, 1 mmol/L $MgCl_2$, 0.002% NP40, 0.01% sodium deoxycholate, and 1 mg/mL 5-bromo-4-chloro-3-indolyl-β-D-galactopyranoside.

Assays of Apoptosis. For Hoechst 33342 staining, cells were grown on coverslips, starved for 15 hours in medium containing 5% FCS, and then treated with VEGF (50 ng/mL) in the presence or absence of luteolin or rapamycin for the same period of time. Cells were fixed in 3.7% paraformaldehyde for 15 minutes, and detection of apoptosis was based on DNA staining with Hoechst 33342 (Molecular Probes, Eugene, OR). Apoptotic nuclei were counted using a Zeiss fluorescence microscope.

For analysis by flow cytometry, HUVECs (infected or uninfected) were serum starved for 15 hours in medium containing 5% FCS and treated with VEGF (50 ng/mL) in the presence or absence of luteolin for the same period of time. At the end of the incubation time, floating and adherent cells were collected in ice-cold PBS, stained with propidium iodide using the CycleTEST

[5] www.coloncancer.org/adeasy.htm.

PLUS DNA Reagent kit (Becton Dickinson Biosciences), and processed for flow cytometric analysis using a Becton Dickinson fluorescence-activated cell scanner. The percentage of cells with a sub-G_1 DNA content was considered as the cell population that had undergone apoptosis.

Evaluation of Proliferation. For analysis by Ki67 immunostaining, HUVECs were grown on coverslips and serum starved in medium containing 5% FCS for 12 hours. Cells were induced with VEGF (50 ng/mL) in the absence or presence of various concentrations of luteolin for 6 hours, fixed in 3.7% paraformaldehyde, and processed for indirect immunofluorescence using an anti-Ki67 antibody as described below. Cells were counterstained with Hoechst 33342. Proliferating cells (Ki67-positive cells) and apoptotic cells (pyknotic nuclei by Hoechst staining) were recognized and counted using a Zeiss fluorescence microscope.

For analysis by [^{3}H]thymidine incorporation, subconfluent adenovirus-infected HUVECs were serum starved in medium containing 5% FCS for 12 hours and then induced for 24 hours with VEGF (50 ng/mL) in the presence or absence of various concentrations of either luteolin or rapamycin. Methyl-[^{3}H]thymidine (1 μCi/mL) was added to each well for the last 6 hours of incubation, culture medium was removed, and the cells were fixed at 4°C for 20 minutes in ice-cold 10% tricloroacetic acid. Samples were subsequently washed three times with H_2O and solubilized in 0.1 N NaOH overnight at 4°C. The radioactivity was counted in a beta liquid scintillation counter (LKB-Wallac, Sweden) and normalized to the number of viable cells. Dead cells were recognized by Hoechst and trypan blue staining and excluded from the counting. Uniform expression of HA-myrAkt in all conditions was confirmed with Western blot analysis.

Indirect Immunofluorescence. Cells were grown on coverslips, infected, and treated for apoptotic assays as described above. Cells were then fixed in 3.7% paraformaldehyde for 15 minutes, quenched with 50 mmol/L ammonium chloride for 15 minutes, and permeabilized with 0.1% Triton X-100 for 4 minutes, and nonspecific sites were blocked with 10% FCS. Primary and secondary antibodies were diluted in 5% FCS. Fluorescein isothiocyanate- or tetramethylrhodamine isothiocyanate-conjugated donkey antimouse and anti-rabbit IgG secondary antibodies were used at a 1:200 dilution. Coverslips were mounted in Mowiol and viewed using a Zeiss fluorescence microscope.

Rabbit Corneal Neovascularization Assay. Corneal assays were performed in New Zealand White rabbits (Charles River, Calco, Lecco, Italy; ref. 23) in accordance with the guidelines of the European Economic Community for animal care and welfare (EEC Law No. 86/609). Briefly, after anesthetization with sodium pentothal (30 mg/kg), slow-release pellets bearing test substances were implanted in micropockets surgically produced in the lower half of the cornea. Subsequent daily observation of the implants was carried out with a slit lamp stereomicroscope. Luteolin was initially tested to ascertain the possible angiogenic and/or inflammatory activity of the compound. Then, the antiangiogenic activity of luteolin was evaluated by implanting in the corneal tissue pellets with $VEGF_{165}$ (200 ng) with or without luteolin (0.5 μg). The eyes were observed for 10 days, and the angiogenic response was recorded. Five eyes for each condition were used in two independent experiments.

A-431 Murine Xenograft Model. To assess the *in vivo* antiangiogenic/antitumor activity of luteolin, female immunodeficient mice (5- to 8-week–old BALB/c nude mice; Harlan Nossan, Milan, Italy) were inoculated subcutaneously in the right flank with 10^7 A-431 cells in a volume of 50 μL (24). After 1 week, when tumors reached a volume of 100 mm^3, animals were randomly assigned to different experimental groups (seven mice per group). Peritumor treatment with luteolin (5 μg/d/mouse) or vehicle was performed. The vehicle containing the same concentrations of solvents (1% EtOH +1% DMSO) was used as control. Daily treatment was performed for 7 consecutive days. Serial caliper measurements of perpendicular diameters were used to calculate tumor volume using the following formula: (shortest diameter × longest diameter × thickness of the tumor in mm). Data are reported as tumor volume in mm^3. Experiments have been performed in accordance with the guidelines of the European Economic Community for animal care and welfare (EEC Law No. 86/609) and National Ethical Committee. Animals were observed daily for signs of cytotoxicity and sacrified by CO_2 asphyxiation.

Upon excision, each tumor was immediately frozen in liquid nitrogen. Seven-micrometer–thick cryostat sections were stained with hematoxylin and eosin, and adjacent sections were used for immunohistochemical staining with the anti–ED-B monoclonal antibody after fixation in cold absolute acetone. Microvessel density was evaluated by randomly counting ED-B positively stained vessel-like structures in three different sections. In each section, seven counts were performed at ×20 magnification. Data (mean ± SE) are reported as the number of total vessel-like structures counted per section.

Statistics. Data from the *in vitro* experiments are expressed as the mean ± SE. Three or more groups were compared by one-way analysis of variance followed by *post hoc* analysis adjusted with least significant difference correction for multiple comparisons. For the rabbit corneal angiogenesis experiment, the nonparametric Mann-Whitney *U* test was used. In the case of the xenograft and microvessel density experiments, statistical analysis was performed using Student's *t* test for grouped data. SSPS software was used in all analyses.

RESULTS

Luteolin Inhibits VEGF-Induced Neovascularization in the Rabbit Cornea Assay. Luteolin has been shown previously to inhibit EC proliferation and *in vitro* angiogenesis (18). To evaluate whether luteolin could inhibit angiogenesis *in vivo*, we used the rabbit cornea angiogenesis assay. Initial experiments, in which pellets containing 1 μg of luteolin were implanted, revealed no macroscopic evidence of inflammation or neovascularization induced by luteolin alone. Pellets containing VEGF (200 ng) elicited a strong angiogenic response (Fig. 1*A*, *left panel*), which was dramatically reduced when the pellets contained both 0.5 μg of luteolin and VEGF (Fig. 1*A*, *right panel*), and this inhibition was statistically significant at all time points (Fig. 1*B*). Thus, luteolin is capable of inhibiting VEGF-induced angiogenesis *in vivo*.

Luteolin Suppresses Angiogenesis and Tumor Growth in the A-431 Murine Xenograft Model. Having shown that luteolin is an inhibitor of angiogenesis in the rabbit corneal angiogenesis assay, we

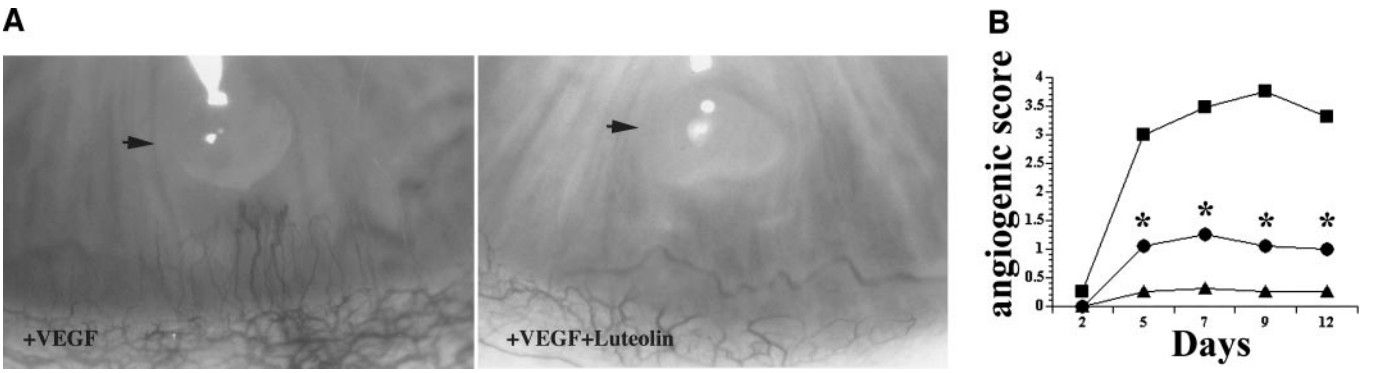

Fig. 1. Luteolin inhibits VEGF-induced *in vivo* angiogenesis (rabbit cornea micropocket assay). *A*, representative pictures of pellets (*arrowheads*) with VEGF (200 ng; *left panel*) or VEGF (200 ng) + luteolin (0.5 μg; *right panel*) implanted in corneal micropockets (7th day of observation). *B*, data presented as angiogenic score over time (days). VEGF, ■; VEGF + luteolin, ●; luteolin, ▲. Angiogenic score = number of vessels × distance from limbus. *, $P < 0.05$ *versus* VEGF-induced angiogenesis (Mann-Whitney *U* test).

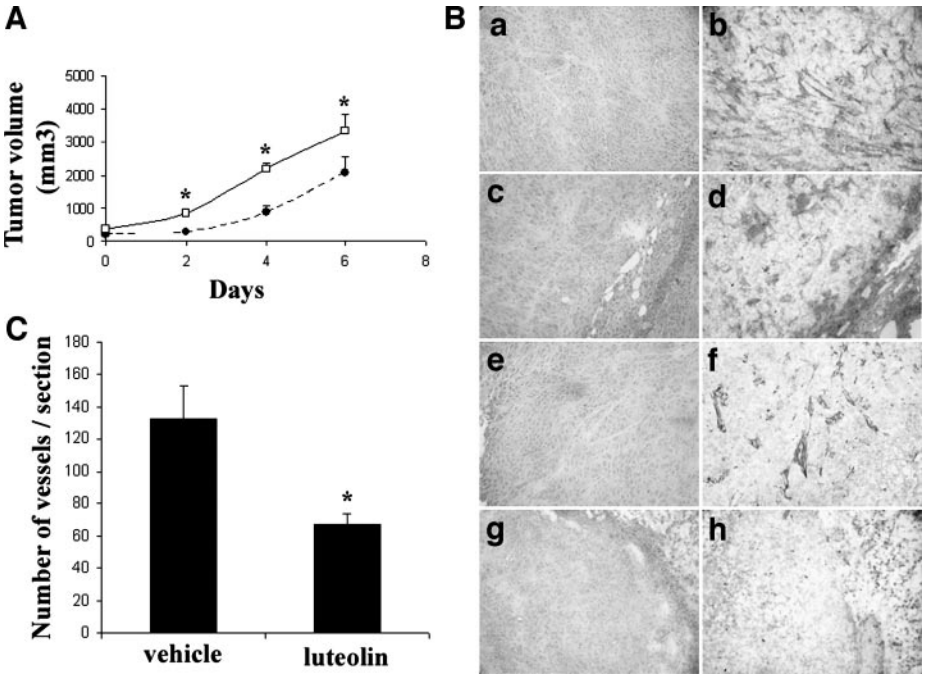

Fig. 2. Luteolin inhibits tumor growth and angiogenesis. *A*, nude mice were inoculated with A-431 cells, and tumors were allowed to reach a volume of approximately 100 mm^3. The tumors were then treated with daily peritumor injections of either luteolin, ● (5 μg/mouse/d), or vehicle, □ (1% EtOH + 1% DMSO), for 7 consecutive days. Serial caliper measurements of perpendicular diameters were used to calculate tumor volume. Data are reported as tumor volume in mm^3 (mean ± SE of at least seven animals per group) over time (days). The differences in tumor volume are statistically significant (*, $P < 0.01$, Student's *t* test). *B*, the effect of luteolin (*e*–*h*) on tumor angiogenesis at day 8 was compared with the vehicle-treated group (*a*–*d*). Representative pictures of tumor core (*a*, *b*, *e*, and *f*) and actively growing tumor periphery (*c*, *d*, *g*, and *h*) stained with hematoxylin and eosin (*a*, *c*, *e*, and *g*) and with an anti–ED-B antibody specific for ED-B of fibronectin (*b*, *d*, *f*, and *h*) are shown. A positive signal was visible in microvessels and in the matrix undergoing remodelling due to tumor cell activity. Magnification, ×40. *C*, on excision, each tumor was immediately frozen in liquid nitrogen. Seven-micrometer–thick cryostat sections were stained with hematoxylin and eosin, and adjacent sections were used for immunohistochemical staining with the anti–ED-B monoclonal antibody after fixation in cold absolute acetone. Microvessel density was evaluated by randomly counting ED-B positively stained vessel-like structures in three different sections. In each section, seven counts were performed at ×20 magnification. Data are presented as the number of ED-B–positive vessel-like structures per section (mean ± SD). *, $P < 0.05$.

wished to address the antiangiogenic activity and, in extension, the antitumor effect of this molecule in a xenograft tumor model. Indeed, treatment of A-431 tumors with luteolin (5 μg/d/mouse) reduced tumor volume approximately 50% compared with the control group treated with vehicle alone ($P < 0.01$ *versus* vehicle group; Fig. 2*A*). The tumor cores of both the vehicle-treated and the luteolin-treated nude mice were analyzed histologically (hematoxylin and eosin staining) and immunohistologically (anti–ED-B antibody staining; Fig. 2*B*). Using the anti–ED-B antibody, a strong and diffuse staining of the tumor stroma was clearly visible in vehicle-treated tumor sections (Fig. 2*B*, *b* and *d*) as compared with the weak staining of tumor sections from luteolin-treated mice (Fig. 2*B*, *f* and *h*). The anti–ED-B antibody recognizes an isoform of fibronectin containing the ED-B, which is known to accumulate around neovascular structures in aggressive tumors and other tissues undergoing angiogenesis and remodeling (25), and has been used previously to highlight actively growing vasculature in sections of A-431 human tumor implants (26). On quantitation of newly formed vessels, vehicle- and luteolin-treated

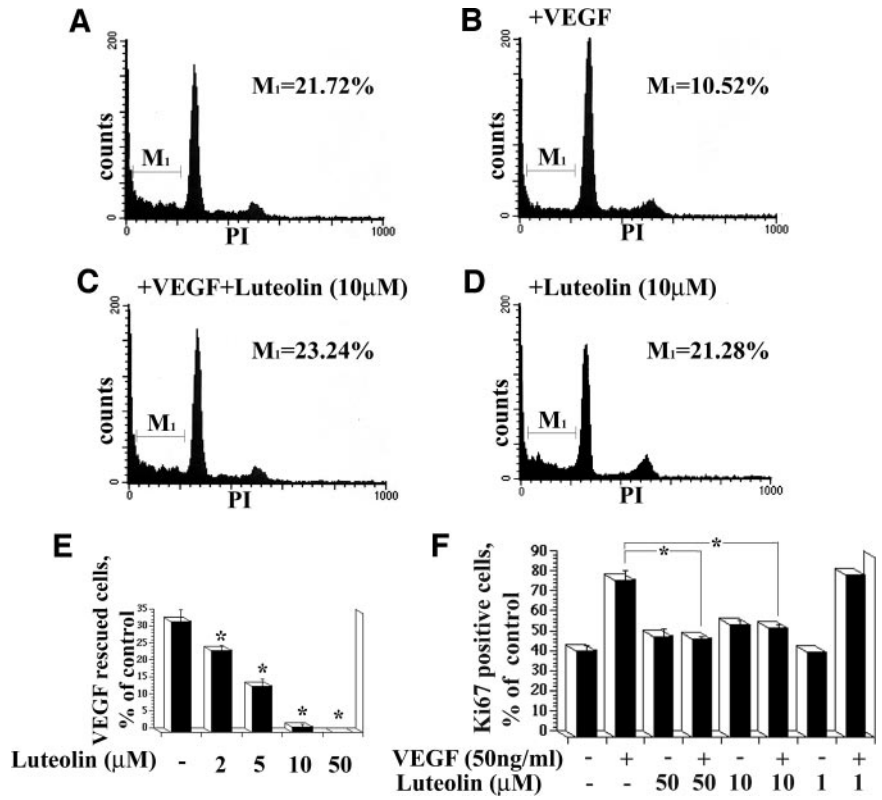

Fig. 3. Luteolin inhibits VEGF-induced survival and proliferation in HUVECs. *A*–*D*, determination of apoptosis by propidium iodide staining and flow cytometry of HUVECs treated with or without VEGF (50 ng/mL) for 15 hours in the presence or absence of 10 μmol/L luteolin. In each panel, the percentage of HUVECs with hypodiploid (apoptotic) DNA content is indicated (M_1). The experiment was carried out five times, and *A*–*D* constitute representative sets of determinations. *E*, percentage of VEGF-rescued cells when HUVECs were cotreated with VEGF (50 ng/mL) and various concentrations of luteolin ($a - b/b \times 100$; a = percentage of apoptotic cells in the presence of different concentrations of luteolin; b = percentage of apoptotic cells in the presence of luteolin and VEGF). The experiment was carried out twice, and *E* represents one representative experiment. *, $P < 0.025$ *versus* control cells; ⁕, $P < 0.05$ *versus* control cells. *F*, serum-starved HUVECs were treated with VEGF (50 ng/mL) for 6 hours in the absence or presence of various concentrations of luteolin. Proliferating HUVECs were identified by Ki67 indirect immunofluorescence. Nuclei were counterstained with Hoechst, and pyknotic (apoptotic) nuclei were excluded. Values were calculated as the number of Ki67-positive cells/the number of cells with intact nuclei (Hoechst staining) × 100. Data represent the mean ± SD of three independent experiments. *, $P < 0.025$.

tumors exhibited 132 ± 21 and 67 ± 7 ED-B–positive vessel-like structures per section, respectively ($P < 0.05$; $n = 6$; Fig. 2*C*). Luteolin did not cause any decrease in survival of the treated mice; at day 4, survival was 100% for the group treated with 5 μg/day luteolin and 90% for vehicle-treated group.

Luteolin Inhibits VEGF-Induced Survival and Proliferation of Endothelial Cells. To elucidate the cellular mechanisms underlying the inhibitory effect of luteolin on VEGF-induced angiogenesis, we investigated the effect of luteolin on VEGF-induced survival and proliferation of HUVECs, two important angiogenic EC responses. Withdrawal of serum is well known to induce EC apoptosis, which is reversible on VEGF addition. Therefore, we have examined the effect of luteolin on VEGF-induced survival of HUVECs. Indeed, whereas serum-starved HUVECs (in 5% FCS) were apoptotic, being hypodiploid by fluorescence-activated cell-sorting (FACS) analysis (Fig. 3*A*), treatment of HUVECs with VEGF for 15 hours rescued 50% of the cells from apoptosis (Fig. 3*B*). Cotreatment with 10 μmol/L luteolin totally inhibited the VEGF-induced EC survival (Fig. 3*C*), and this effect was dose dependent (Fig. 3*E*). Furthermore, luteolin did not further increase the level of apoptosis of the serum-deprived HUVECs, excluding the possibility of toxic or apoptotic effects of luteolin itself (Fig. 3*D*). Identical results were obtained when we analyzed luteolin-treated cells by terminal deoxynucleotidyl transferase-mediated nick end labeling or Hoechst 33342 staining (data not shown). To determine whether luteolin could also directly inhibit VEGF-induced proliferation, serum-starved HUVECs were treated with VEGF for 6 hours, and proliferating cells were identified (cells expressing the Ki67 antigen and simultaneously exhibiting intact, nonpyknotic nuclei). Ki67 antigen is only expressed in active phases of the cell cycle, but not in G_0 phase (27), and the percentage of the Ki67-positive cells represents the proliferating population. VEGF doubled the percentage of Ki67-positive HUVECs, compared with the nontreated cells, and this increase was inhibited strongly and in a dose-dependent manner when HUVECs were cotreated with various concentrations of luteolin (Fig. 3*F*).

Luteolin Partially Inhibits VEGF-Induced Phosphorylation and Kinase Activation of VEGFR-2. To identify the exact point of luteolin interception on the signaling cascades of VEGF that regulate survival and proliferation of HUVECs, we first investigated the effect of luteolin on VEGF-induced VEGFR-2 activation. VEGFR-2 has been shown to play a principal role in the transduction of VEGF-mediated signals regulating survival and proliferation of ECs. After VEGF treatment for 5 minutes of serum-starved HUVECs, the phosphorylation state and the kinase activity of the VEGFR-2 were assessed by immunoprecipitation of the receptor followed by phosphotyrosine immunodetection or *in vitro* kinase assay. Indeed, VEGF increased tyrosine autophosphorylation of a 230-kDa band, which corresponds to VEGFR-2 (Fig. 4*A*–*C*, *Lane 2*). Cotreatment of HUVECs with 50 μmol/L luteolin partially inhibited the VEGF-induced tyrosine phosphorylation and kinase activity of the receptor (Fig. 4*A* and *B*, *Lane 3*), whereas 10 μmol/L luteolin exhibited no effect (Fig. 4*C*, *Lane 3*). Luteolin alone exerted no effect on VEGFR-2 phosphorylation (Fig. 4*A* and *B*, *Lane 4*). Because luteolin may be lost at the immunoprecipitation step, and its concentration may be very low during the *in vitro* kinase assay, we have repeated the *in vitro* kinase assays of VEGFR-2 adding 10 or 50 μmol/L concentrations of luteolin to the immunoprecipitates before carrying out the kinase assays. Whereas luteolin inhibited the kinase activity of VEGFR-2 at 50 μmol/L (Fig. 4*D*, *Lane 3*), 10 μmol/L concentrations of the compound were devoid of any appreciable effect (Fig, 4*D*, *Lane 4*). Thus, luteolin inhibits VEGF-induced phosphorylation and activation of VEGFR-2 at doses much higher than those inhibiting VEGF-induced survival and proliferation of HUVECs.

Luteolin Inhibits VEGF-Induced Phosphorylation of Akt, Enhances Phosphorylation of p38 MAPK, and Does Not Affect Phosphorylation of ERK1/2 MAPKs. Because luteolin inhibited VEGF-induced phosphorylation and activation of VEGFR-2 at doses much higher than those inhibiting VEGF-induced survival and proliferation

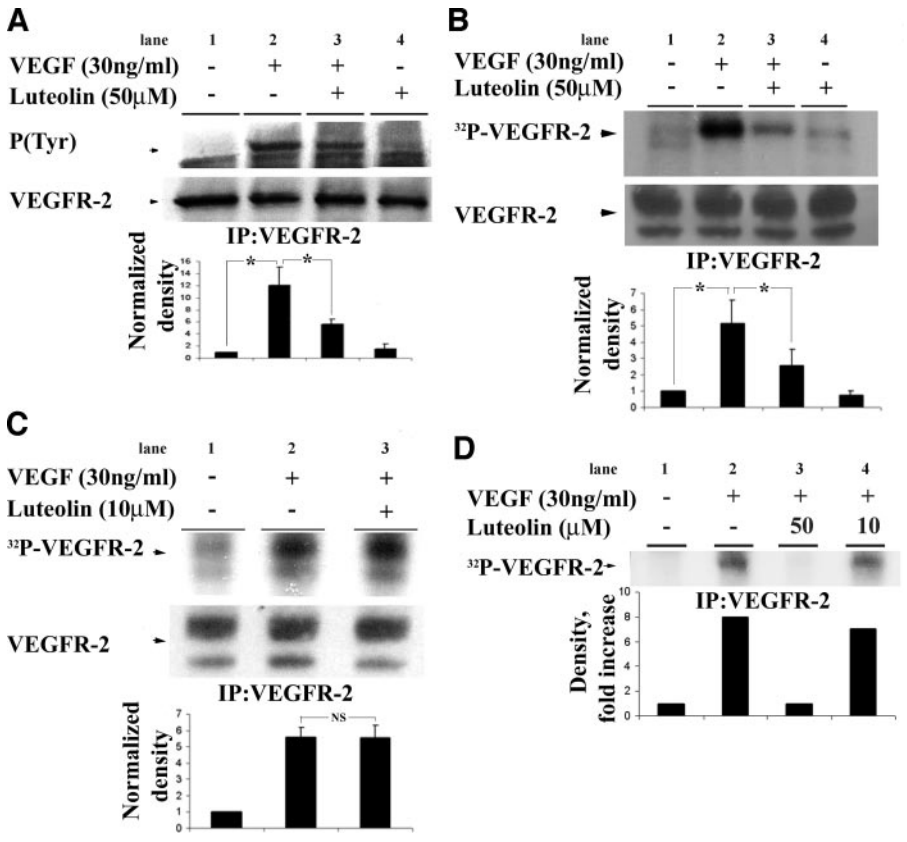

Fig. 4. Luteolin partially inhibits VEGFR-2 activation at 50 μmol/L, but not at 10 μmol/L. *A*–*C*. Serum-starved HUVECs were treated with VEGF (30 ng/mL) in the presence or absence of 50 or 10 μmol/L luteolin for 5 minutes. VEGFR-2 was immunoprecipitated from solubilized cell extracts with a polyclonal anti–VEGFR-2 antibody, and VEGFR-2 phosphorylation was determined either by immunoblotting with an anti–phospho-tyrosine antibody (*A*) or by kinase assay (*B* and *C*). Equal amounts of the receptor in all of the samples were confirmed by Western blot analysis (*bottom panel* in each section of the figure). The experiments were carried out four times, and representative autoradiograms and Western blots are presented. Densitometric normalization of VEGFR-2 phosphorylation against VEGFR-2 band density is shown in *columns*. *, $P < 0.025$; *NS*, nonsignificant. *D*. Serum-starved HUVECs were treated with VEGF (30 ng/mL). Cells were lysed, and VEGFR-2 was immunoprecipitated as described above. The immunoprecipitates from VEGF-treated cells were divided in three equal parts, to which either 10 or 50 μmol/L luteolin or DMSO/EtOH (solvent control) was added, and kinase assays were carried out. Representative autoradiogram and quantification of band intensities are shown in *columns*.

of HUVECs, we sought downstream mediators of VEGF signals as potential targets of the action of luteolin. VEGF induces survival of ECs mainly via the activation of Akt (15), whereas activation of ERK1/2 MAPKs is thought to be essential for VEGF-induced proliferation (28). To assess the effect of luteolin on these pathways, serum-starved HUVECs were treated with VEGF for 15 minutes in the presence or absence of luteolin, and cell lysates were subjected to immunodetection using antibodies against either phosphorylated Akt (Ser^{473}) or phosphorylated ERK1/2. As expected, VEGF enhanced the phosphorylation status of Akt (Fig. 5*A*, *Lanes 2* and *6*) and ERK1/2 (Fig. 5*B*, *Lane 2*). Cotreatment with luteolin completely abolished VEGF-stimulated phosphorylation of Akt at both 50 μmol/L (Fig. 5*A*, *Lane 7*) and 10 μmol/L (Fig. 5*A*, *Lane 3*) concentrations. In contrast, luteolin was unable to inhibit VEGF-induced ERK1/2 phosphorylation even at 50 μmol/L (Fig. 5*B*, *Lane 4*). In light of the efficient inhibition of Akt activation by luteolin, we have examined the effect of this compound on p38 phosphorylation. It has been shown previously that VEGF can stimulate the Akt and MAPK kinase (MKK) 3/MKK6/p38 pathways, which are linked to survival and apoptosis of ECs, respectively (15, 29, 30). Because Akt down-regulates p38 activation, blockade of the Akt pathway enhances VEGF activation of p38 and apoptosis (30). Consistent with these studies, luteolin enhanced VEGF-induced p38 phosphorylation (Fig. 5*C*, *Lanes 3* and *5*) and also could induce p38 phosphorylation alone (Fig. 5*C*, *Lanes 4* and *6*), both in a dose-dependent manner. Induction of p38 phosphorylation in the absence of VEGF is attributed to luteolin-induced inhibition of basal levels of Akt activity. Moreover, overexpression of myrAkt inhibited VEGF-induced phosphorylation of p38 and blocked the effect of luteolin on p38 phosphorylation, confirming that this effect was through Akt (Fig. 5*D*). Taken together, these results suggest that inhibition of VEGF-induced Akt phosphorylation plays a key role in the apoptotic activity of luteolin on VEGF-treated HUVECs. Luteolin not only inhibits downstream effects of the Akt survival pathway but also, via Akt blockade, allows overactivation of the MKK3/MKK6/p38 apoptotic pathway of VEGF, eliciting strong apoptotic death in HUVECs.

Luteolin Inhibits VEGF-Induced Activity of PI3K. Because Akt activation was inhibited by luteolin, we have investigated the effect of luteolin on VEGF-induced stimulation of PI3K, a lipid kinase that has been shown to be the main upstream activator of Akt (31, 32). Serum-starved HUVECs were stimulated with VEGF in the presence or absence of luteolin, and PI3K was immunoprecipitated using an antibody against the p85 regulatory domain of PI3K. The samples were then subjected to *in vitro* PI3K assays using phosphatidylinositol 4,5-diphosphate as substrate. As expected, VEGF induced the lipid kinase activity of PI3K as judged by phosphatidylinositol 3,4,5-triphosphate production (Fig. 6*A*, *Lanes 2* and *6*). Luteolin inhibited VEGF-induced PI3K activity at both 50 (Fig. 6*A*, *Lane 3*) and 10 μmol/L (Fig. 6*A*, *Lane 7*). Moreover, luteolin was capable of inhibiting basal levels of PI3K activation at 50 μmol/L (Fig. 6*A*, *Lane 4*). Similar results were obtained when serum-deprived cells were stimulated with VEGF and luteolin was added to the immunoprecipitates before the *in vitro* PI3K assay (Fig. 6*B*). These data demonstrate that

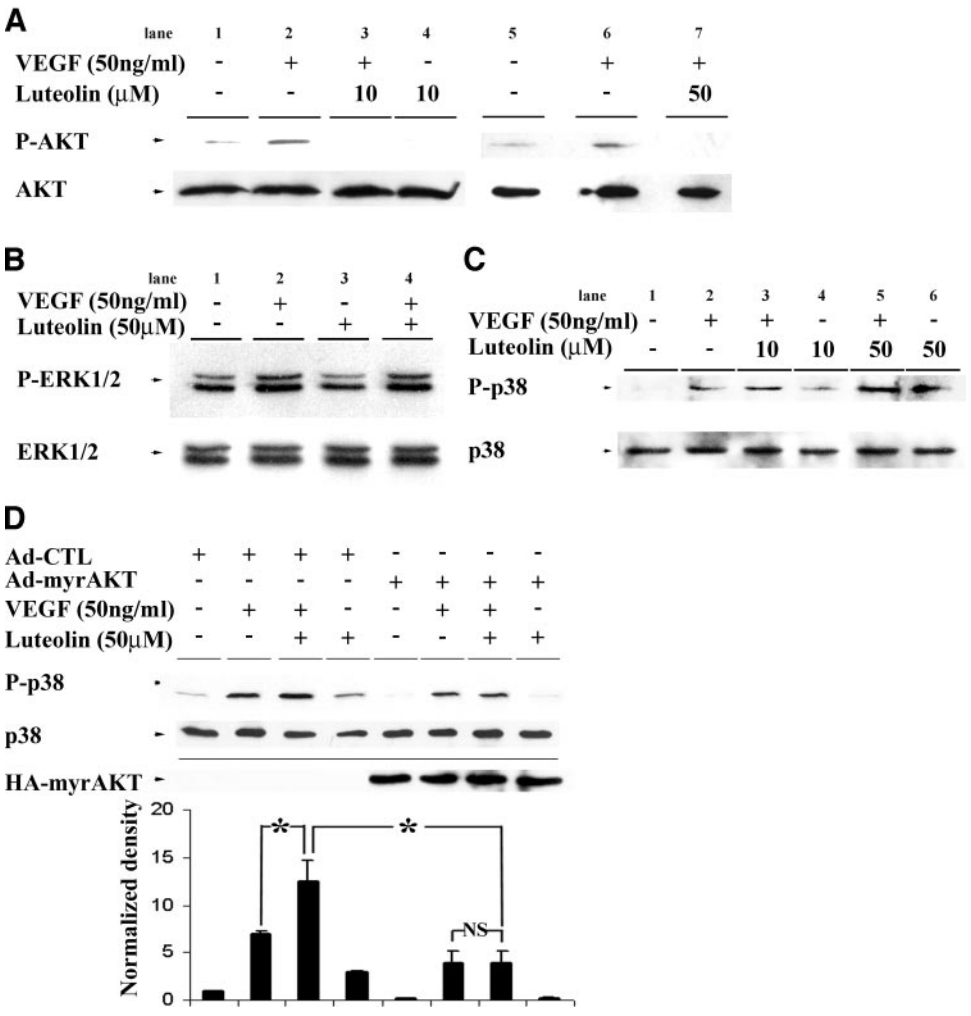

Fig. 5. Luteolin inhibits VEGF-induced phosphorylation of Akt and enhances phosphorylation of p38 MAPK. *A*−*C*. Serum-starved HUVECs were treated with VEGF (50 ng/mL) in the presence or absence of luteolin for 15 minutes. Equal amounts of total cell lysates were analyzed by Western blot analysis for phospho-Akt and Akt (*A*), phospho-ERKs and ERKs (*B*), and phospho-p38 and p38 (*C*). *D*. HUVECs were infected with adenoviruses expressing HA-myrAkt (Ad-myrAkt) or β-galactoside (Ad-CTL) for 2 hours. After 30 hours in full medium, cells were serum-starved for 12 hours and treated with VEGF (50 ng/mL) in the presence or absence of luteolin for 15 minutes. Equal amounts of total cell lysates were analyzed by Western blot analysis for phospho-p38, p38, and HA-myrAkt. Densitometric normalization of phosphorylated p38 against p38 band density is shown in *columns*. All Western blot analyses in *A*−*D* were perfomed twice. *, $P < 0.025$; *NS*, nonsignificant.

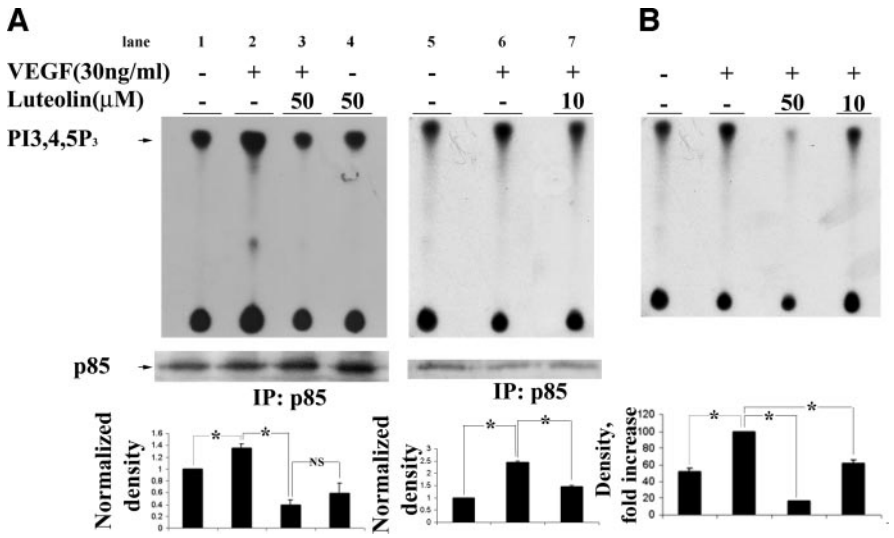

Fig. 6. Luteolin inhibits VEGF-induced PI3K activity. *A*. Serum-starved HUVECs were treated with VEGF (50 ng/mL) in the presence or absence of luteolin for 15 minutes. PI3K was immunoprecipitated with a polyclonal antibody against the regulatory subunit p85 and assayed for ability to phosphorylate 4,5-phosphatidylinositol phospholipid. Representative autoradiograms ($n = 3$) and quantification of the phosphorylated lipid products (densitometric normalization of lipid spots against the p85 band density for each sample in columns) are shown .*, $P < 0.025$; *NS*, nonsignificant. *B*. Serum-starved HUVECs were treated with VEGF (30 ng/mL). PI3K was immunoprecipitated as described above. The immunoprecipitates from VEGF-treated cells were divided in three equal parts, to which either 10 or 50 μmol/L luteolin or DMSO/EtOH (solvent control) was added, and lipid kinase assays were carried out. Representative autoradiogram and quantification of the product band intensities are shown. *, $P < 0.025$.

inhibiton of PI3K represents the main molecular target of luteolin in VEGF-treated HUVECs.

Constitutively Active Akt Rescues Endothelial Cells from the Antisurvival Effect of Luteolin, Whereas It Weakly Reverses the Effect of Luteolin on VEGF-Induced Proliferation. To confirm the central role of the PI3K/Akt pathway as a target of the apoptotic effect of luteolin, we have infected HUVECs with an adenovirus expressing a constitutively active form of Akt (myrAkt), which targets the protein to the cell membrane independently of prior activation by PI3K (33). Infected cells were serum starved and stimulated with VEGF in the presence or absence of luteolin, and the level of apoptosis was assayed by FACS analysis. Infected cells expressing myrAkt were considerably more resistant to apoptosis induced by serum withdrawal compared with cells infected with the control virus (Fig. 7*A*, *columns 1* and *5*). Luteolin, even at 50 μmol/L, was unable to cause apoptosis in cells infected with Ad-myrAkt, irrespective of whether they were treated with VEGF or not (Fig. 7*A*, *columns 7* and *8*). In contrast, luteolin could maintain its apoptotic effects on HUVECs infected with the control virus (Fig. 7*A*, *columns 3* and *4*). The results were essentially the same when apoptosis was evaluated by the appearance of pyknotic nuclei by fluorescence microscopy (Hoechst staining; data not shown). Thus, it can be firmly concluded that luteolin inhibits the VEGF-induced survival effect on HUVECs via blockade of the PI3K/Akt pathway.

Because activation of Akt is implicated in cell proliferation (34, 35), we investigated whether expression of myrAkt also would rescue the effect of luteolin on VEGF-induced proliferation of HUVECs. Whereas luteolin strongly inhibited VEGF-induced incorporation of thymidine at 10 and 50 μmol/L in HUVECs infected with control adenoviruses (Fig. 7*B*, *columns 2* and *3*), the effect was only weakly rescued in HUVECs infected with the adenoviruses expressing myrAkt (Fig. 7*B*, *columns 5* and *6*), without reaching statistical significance. Thus, blockade of Akt by luteolin does not contribute considerably to the inhibitory effect of luteolin on VEGF-induced proliferation of HUVECs.

Luteolin Inhibits VEGF-Induced Phosphorylation of p70 S6 Kinase. Because Akt seems to play a minor role in the antiproliferative effect of luteolin, we investigated the effect of luteolin on p70 S6K activation, another effector of PI3K, which has been shown to play a role in VEGF-induced proliferation in HUVECs (13). Indeed, we show here that p70 S6K was phosphorylated by VEGF at Thr^{389} (Fig. 7*C* and *F*, *Lanes 2*), one of the important phosphorylation sites for activation of p70 S6K *in vivo* (36). Phosphorylation of Thr^{389} was inhibited by rapamycin (Fig. 7*C*, *Lane 3*), a compound that inhibits FKBP 12-rapamycin-associated protein (FRAP), an upstream activator of p70 S6K. Consistent with these results, VEGF-induced thymidine incorporation in HUVECs was rapamycin sensitive, even after overexpression of myrAkt (Fig. 7*D*), whereas the survival effect of VEGF on HUVECs was rapamycin insensitive (Fig. 7*E*). Moreover, rapamycin did not inhibit VEGF-induced ERK phosphorylation (data not shown). Taken together, these results reserve a key role for p70 S6K activation on the mitotic effects of VEGF in HUVECs. Luteolin, both at 50 and 10 μmol/L, completely inhibited VEGF-induced phosphorylation of p70 S6K at Thr^{389} (Fig. 7*F*, *Lanes 4* and *5*). This result strongly suggests that the antimitotic effect of luteolin on VEGF-induced proliferation of HUVECs is mediated mainly via inhibition of p70 S6K activation.

DISCUSSION

In an attempt to identify phytochemicals contributing to the well-documented preventive effect of plant-based diets on cancer incidence and mortality (16, 17), we have shown previously (18) that certain isoflavonoids and flavonoids inhibit proliferation of cultured tumor cells and *in vitro* angiogenesis. In agreement with our results, the isoflavonoid genistein, as well as two flavonoids, fisetin and luteolin, inhibited fibroblast growth factor-2–induced angiogenesis using the rabbit corneal neovascularization assay (37). Here we show that luteolin inhibits VEGF-induced angiogenesis in the rabbit cornea. This is the first study showing inhibition of VEGF-induced angiogenesis *in vivo* by a single flavonoid. Previously, inhibition of VEGF-induced angiogenesis has been seen using green tea extracts rich in certain flavonoids, such as epigallocatechin-3-gallate (38). The antiangiogenic activity of luteolin was further confirmed in a murine tumor xenograft model using A-431 cells, a human epidermoid carcinoma cell line that produces VEGF (39). In this system, luteolin significantly reduced angiogenesis of the xenograft tumors, and this was associated with a reduced tumor volume in the luteolin-treated mice. It is therefore reasonable to assume that inhibiton of angiogenesis is a postinitiation effect of luteolin and perhaps other flavonoids, potentially contributing to the protective effect of plant-based diets on cancer. Indeed, in a recent study, whereas tumor incidence and multiplicity were not affected, a significant reduction in the tumor volumes of 7,12-dimethylbenz(*a*)anthracene/12-*O*-tetradecanoylphorbol-13-acetate–induced skin papillomas was obseved after oral administration of luteolin-rich perilla leaf extracts in mice (40). In

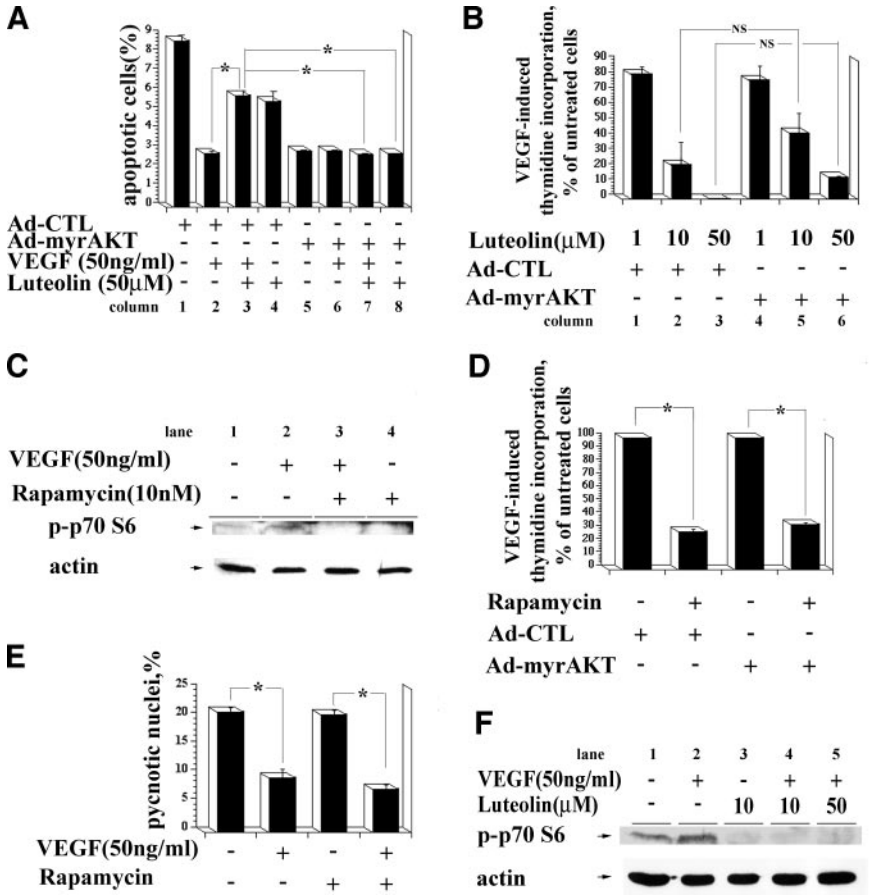

Fig. 7. Constitutively active Akt rescues ECs from the antisurvival effect of luteolin while weakly reversing the effect of luteolin on VEGF-induced proliferation. *A*. HUVECs were infected with adenoviruses expressing HA-myrAkt (Ad-myrAkt) or β-galactosidase (Ad-CTL) for 2 hours. After 30 hours in full medium, cells were serum starved and treated with VEGF (50 ng/mL) in the presence or absence of luteolin for 15 hours. The percentage of cells with hypodiploid DNA content, as determined by propidium iodine staining and flow cytometry, is shown. The experiment was performed twice. *, $P < 0.025$. *B*. HUVECs were infected as described in *A*, serum starved, and induced with VEGF in the presence or absence of various concentrations of luteolin for 24 hours. [^{3}H]Thymidine was added for the last 6 hours of incubation, and the radioactivity measured (indicating DNA synthesis) was normalized to viable cells. Values shown are calculated as VEGF-induced thymidine incorporation in cells treated with various concentrations of luteolin expressed as a percentage of the VEGF-induced thymidine incorporation in cells treated only with VEGF. The experiment was performed three times in triplicate, and the results presented are from one representative experiment. *NS*, the correlation is not statistically significant. *C*. Serum-starved HUVECs were treated with VEGF (50 ng/mL) in the presence or absence of rapamycin for 15 minutes. Equal amounts of total cell lysates were analyzed by Western blot analysis for phospho-Thr^{389}-p70 S6K. Equal loading was confirmed by reprobing the blot with an antiactin antibody. The experiment was performed twice. *D*. HUVECs were infected as described above, serum starved, and induced with VEGF in the presence or absence of rapamycin for 24 hours. [^{3}H]Thymidine was added for the last 6 hours of incubation, and the radioactivity measured (indicating DNA synthesis) was normalized to viable cells. Values shown are calculated as VEGF-induced thymidine incorporation in cells treated with rapamycin expressed as a percentage of the VEGF-induced thymidine incorporation in cells treated only with VEGF. The experiment was performed twice in triplicate. *, $P < 0.025$. *E*. HUVECs grown on coverslips were serum starved and induced with VEGF (50 ng/mL) in the presence or absence of 10 nmol/L rapamycin for 15 hours, and the percentage of pyknotic (apoptotic) nuclei (Hoechst-stained nuclei) was calculated. The experiment was carried out twice. *, $P < 0.025$. *F*. Serum-starved HUVECs were treated with VEGF (50 ng/mL) in the presence or absence of luteolin 50 and 10 μmol/L for 15 minutes. Equal amounts of total cell lysates were analyzed by Western blot analysis for phospho-Thr^{389}-p70 S6K. Equal loading was confirmed by reprobing the blot with an antiactin antibody. The experiment was performed twice.

agreement with the inhibiton of angiogenesis *in vivo*, luteolin inhibited VEGF-induced survival of cultured HUVECs in a dose-dependent manner at a half-maximal concentration of 4 μmol/L. Moreover, luteolin inhibited VEGF-induced proliferation of ECs independently from its effects on survival. Taken together, these results strongly suggest that luteolin is capable of inhibiting VEGF-dependent responses of ECs.

Because flavonoids are competitive inhibitors of ATP binding (41) and inhibit several tyrosine and serine kinases (41, 42), we have considered the kinase activities of VEGFR-2 and downstream pathways as possible molecular targets of luteolin. Luteolin partially inhibited VEGF-induced VEGFR-2 phosphorylation only at 50 μmol/L. Because luteolin inhibits VEGF-induced survival and proliferation of ECs at concentrations below 10 μmol/L, inhibition of the tyrosine kinase activity of VEGFR-2 could not have been responsible for the action of luteolin, and the interception point of luteolin had to be sought at the level of downstream kinases.

Toward this end, we show here that luteolin strongly inhibited VEGF-induced phosphorylation of Akt at 10 μmol/L and that overexpression of a constitutively active form of Akt rescues ECs from the antisurvival effect of luteolin. Evidently, luteolin, via inhibiton of Akt activation, influences downstream effectors of apoptosis, such as BAD, caspase 9, and Forkhead transcription factor (43). Akt effectors, such as the FRAP (called also mammalian target of rapamycin), which regulate survival via modulation of surface transporters for extracellular nutrients (44), seem to be less important in HUVECs because the effect of VEGF on survival in these cells was rapamycin insensitive. Also, luteolin did not influence EC survival via interference with nuclear factor (NF)-κB activation. We did not observe any NF-κB activation by VEGF in ECs in either the absence or presence of luteolin (data not shown). Akt can stimulate the RelA/p65 transactivation subunit of NF-κB in an IκB kinase-dependent manner (45), eliciting cell survival via NF-κB gene transcription (46). Interestingly, luteolin enhanced VEGF-induced phosphorylation of p38 in HUVECs, a pathway that is known to cause apoptosis in ECs (47, 48). Evidently, because Akt down-regulates p38 activation (30), inhibition

of the Akt pathway by luteolin enhances VEGF-induced phosphorylation of p38. Indeed, overexpression of a constitutively active form of Akt abolishes the effect of luteolin on VEGF-induced p38 phosphorylation. Thus, luteolin, via Akt blockade, not only inhibits downstream survival signals but also enhances the proapoptotic MKK3/MKK6/p38 pathway of VEGF, eliciting a strong apoptotic effect in ECs.

Activation of Akt requires translocation of the kinase from the cytosol to the plasma membrane. This process depends on the catalytic activity of PI3K, which results in phospholipid products that are recognized by the pleckstrin homology domain of Akt (49). After translocation to membranes, Akt is activated by phosphorylations at Ser^{473}, by an unknown kinase or autophosphorylation, and at Thr^{308}, by 3-phosphoinositide-dependent protein kinase 1 (PDK 1; ref. 50). Here we show that luteolin inhibits VEGF-induced PI3K activity at concentrations similar to those exerting antisurvival and antimitotic effects in ECs. Because certain flavonoids can inhibit PI3K activity *in vitro* by binding to its ATP binding pocket (51), the result implies a direct effect of luteolin on the catalytic activity of PI3K. Alternatively, luteolin could inhibit phosphorylation of the p85 subunit of PI3K, although it is controversial whether such phosphorylation is required for activation of the p110 catalytic subunit (52, 53). However, we did not observe induction of p85 phosphorylation by VEGF in ECs or effects of luteolin thereof (data not shown). In either case, the activity of PI3K is the primary target of luteolin, and inhibition of Akt is a consequence of this effect.

With regard to VEGF-induced mitogenesis, luteolin, at 10 μmol/L, did not affect VEGF-induced phosphorylation of ERK1/2 but completely inhibited VEGF-induced phosphorylation of p70 S6K on Thr^{389} in HUVECs. This was surprising because the ERK pathway is considered to play a central role concerning the mitogenic effects of VEGF (28), although there are reports implicating activation of the p70 S6K pathway (13). The serine/threonine kinase p70 S6K phosphorylates the 40 S ribosomal protein S6, which modulates the translation of a mRNA subset that encodes ribosomal proteins and translation elongation factors (54) and supports progression through the G_1 phase of the cell cycle and cell growth (55). Activation of p70 S6K is regulated by phosphorylation of seven different residues, and the phosphorylation status of Thr^{229} and Thr^{389} is intimately linked to PI3K activity (56, 57). Thus, inhibition of PI3K activity by luteolin could play a critical role also in the inhibitory effects of the compound on VEGF-induced proliferation via blockade of the PI3K/p70 S6K pathway.

The mechanism by which PI3K activates p70 S6K is not yet fully understood, but several reports implicate FRAP in this activation. Because Akt has been shown to phosphorylate FRAP (58), and FRAP is capable of phosphorylating p70 S6K on Thr^{389} (59), activation of p70 S6K by PI3K appears to be, at least in part, Akt-dependent. However, although VEGF-induced proliferation in HUVECs was senstitive to rapamycin, an inhibitor of p70 S6K activation by FRAP (60), expression of a constitutively active Akt weakly rescued the inhibitory effect of luteolin, suggesting that PI3K-induced p70 S6K activation occurs in HUVECs mainly via Akt-independent mechanisms. Our observation is in agreement with studies in which kinase-dead mutants of Akt did not inhibit FRAP-dependent p70 S6K activation by growth factors, questioning the contribution of Akt in this process (61). Recent data provide evidence for Akt-independent mechanisms regarding p70 S6K activation by PI3K. Indeed, the p85 regulatory subunit of PI3K can control p70 S6K activation by mediating the formation of a ternary complex with p70 S6K and FRAP (62). In this context, it has been shown that protein phosphatase 2A (PP2A) associates with and dephosphorylates p70 S6K, whereas FRAP inhibits the PP2A-mediated dephosphorylation of Thr^{389} (63), maintaining p70 S6K in the phosphorylated active form (Fig. 8). In

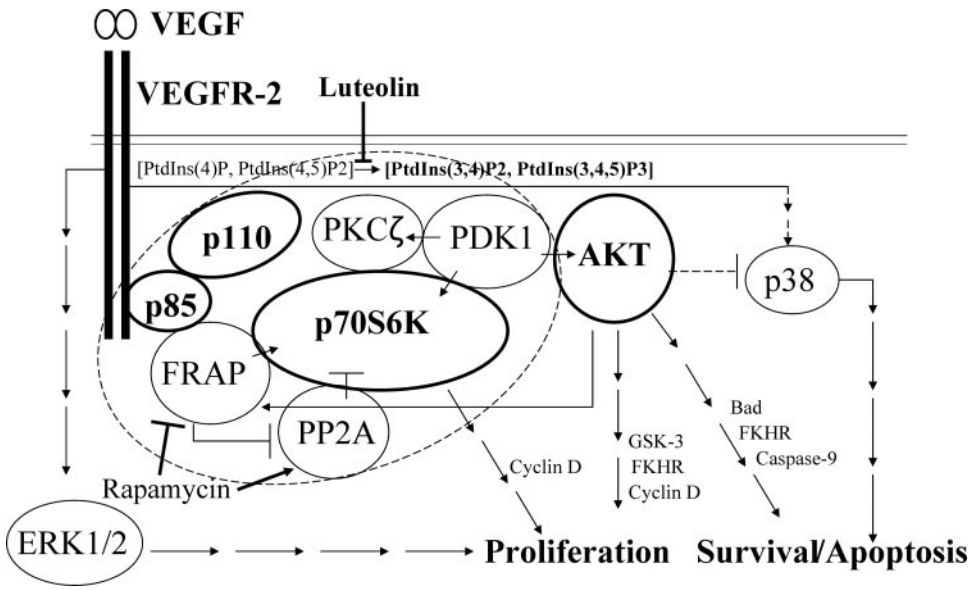

Fig. 8. Flow diagram of the consequences of PI3K inhibition by luteolin on signaling cascades of VEGF regulating survival and proliferation in ECs. Binding of VEGF to VEGFR-2 recruits PI3K via its p85 subunit and activates its p110 catalytic subunit to phosphorylate phosphatidylinositols at position 3. The modified lipids are recognized by the pleckstrin homology domains of PDK1 and Akt, which are recruited to membranes where PDK1 phosphorylates and activates Akt. Additionally, PDK1 phosphorylates and activates p70 S6K, assisted by PKCζ, all three of which are in a complex. The p85 subunit maintains phosphorylations on Thr^{389} of p70 S6K by recruiting FRAP, which inhibits PP2A, a phosphatase that dephosphorylates Thr^{389} of p70 S6K. Luteolin inhibits the catalytic activity of PI3K, thereby abolishing phosphorylation and activation of both Akt and p70 S6Ks. Akt is known to mediate both survival and mitogenic signals, whereas p70 S6K is important for G_1 progression. Expression of constitutively active Akt rescues only the inhibitory effect of luteolin on apoptosis, indicating that the proliferative pathways of Akt, including phosphorylation of p70 S6K on Thr^{389} via FRAP activation, are not important for VEGF-induced mitogenesis in HUVECs. Thus, VEGF induces survival of HUVECs via PI3K- and Akt-dependent pathways, whereas VEGF-induced proliferation appears to proceed via PI3K-dependent, Akt-independent activation of p70 S6K. Indeed, VEGF-induced proliferation of HUVECs is luteolin and rapamycin senstitive. In this context, luteolin did not inhibit VEGF-induced activation of ERK1/2 MAPKs, indicating that its antimitotic effect proceeded almost exclusively via inhibiton of PI3K. On the contrary, phosphorylation of p38 MAPK was enhanced by luteolin, as a consequence of the suppressive effect of Akt on p38, allowing overactivation of the proapoptotic MKK3/MKK6/p38 pathway of VEGF that contributes to the antisurvival effects of luteolin. FKHR, Forkhead transcription factor.

this respect, p85 could maintain phosphorylations that depend on the p110 subunit, which catalyzes the production of 3-phosphorylated phosphatidylinositols that recruit PDK1 (64), which, in turn, phosphorylates p70 S6K on Thr^{229} (65) and Thr^{389}, assisted also by protein kinase C (PKC) ζ and autophosphorylation (66). In agreement with the above, PKCζ and other isoforms of PKC are activated by VEGF in a phospholipase C γ-independent (67) and PI3K-dependent manner (67) and influence VEGF-induced mitogenesis partly via ERK1/2-independent mechanisms (67).

The effects of luteolin on VEGF-induced survival and proliferation were elicited at a half-maximal concentration of ~5 μmol/L. Also, the effects on PI3K and its downstream effectors were active around the same concentrations of luteolin. Are these concentrations achievable in vegetarians, a group benefited by the anticancer preventive effect of plant-based diets? The total flavonoid intake in the United States is calculated to be approximately 1g/day per person (68). The concentrations of intact flavonoids in human plasma are about 1 μmol/L when the quantities of flavonoids ingested do not exceed those commonly obtained from a normal Western diet (69). The content of flavonoids in the diet of vegetarians is expected to be much higher. For instance, the excretion of the isoflavonoid genistein in urine of vegetarians is 30-fold compared with that of omnivores (70). Moreover, the plasma concentration of individual flavonoids ranged from 5 to 14 μmol/L after a single ingestion of orange juice (8 mL/kg) or 300 mL of green tea (71, 72). Thus, regular supply of flavonoids in the diet can maintain flavonoid plasma concentrations at considerable levels (73).

However, the concentration of a specific phytochemical is probably not solely responsible for the protective effects of plant-based diet on cancer incidence. Perhaps luteolin is complemented by several other flavonoids or phytochemicals in achieving significant inhibition of VEGF-induced PI3K activation. Indeed, because flavonoids inhibit several kinases by competing with ATP for binding to the conserved ATP pocket, other flavonoids might also inhibit PI3K as shown for quercetin and myricetin (51). Moreover, low-level inhibition of PI3K by luteolin might be complemented by low-level inhibition of other VEGF effectors by other phytochemicals, leading eventually to effective inhibition of VEGF-induced angiogenesis. Certainly, other flavonoids or phytochemicals might contribute by affecting other characteristics of tumor cells, such as proliferation and apoptosis (18, 19). The present study shows that PI3K and VEGF-induced angiogenesis are among the targets underlining the protective effect of phytochemicals in cancer.

In conclusion, we have observed that luteolin inhibited A-431 xenograft tumor growth and angiogenesis in mice. In agreement, luteolin inhibited VEGF-induced angiogenesis in the rabbit cornea as well as survival and proliferation of HUVECs *in vitro*. Inhibition of the catalytic activity of PI3K by luteolin played an important role in both the antimitotic and apoptotic effects of the compound. Inhibition of PI3K by luteolin affected survival via PI3K/Akt pathways, whereas VEGF-induced proliferation was affected via PI3K/p70 S6K pathways. The results shed light on the mechanisms of action of phytochemicals, such as flavonoids, which might explain the protective action of plant-based diets on the incidence of cancer. Moreover, it might provide the basis of development of more potent synthetic analogs for the inhibition of VEGF-induced angiogenesis.

ACKNOWLEDGMENTS

The skillful technical assistance of Lambrini Kyrkou and Fanny Tahmatzoglou (University of Ioannina, Greece) is gratefully acknowledged. From the University of Ioannina, Greece, we thank Dr. Constantinos Tellis for assistance with thin layer chromatography, Associate Prof. Alexandros Tselepis for use of the FACS facility, and Prof. Kosmas Ferentinos for assistance with statistical analyses. We also thank Philogen S. p. A. Monteriggioni-Siena for providing anti–ED-B antibody. The contribution of Raffaella Solito, (University of Siena, Italy) in the analysis of the xenograft tumors from mice is thankfully acknowledged.

REFERENCES

1. Folkman J. Influence of geometry on growth of normal and malignant cells. Adv Pathobiol 1976;4:12–28.
2. Ferrara N, Gerber HP. The role of vascular endothelial growth factor in angiogenesis. Acta Haematol 2001;106:148–56.
3. Shweiki D, Itin A, Soffer D, Keshet E. Vascular endothelial growth factor induced by hypoxia may mediate hypoxia-initiated angiogenesis. Nature (Lond) 1992;359:843–5.
4. Shweiki D, Neeman M, Itin A, Keshet E. Induction of vascular endothelial growth factor expression by hypoxia and by glucose deficiency in multicell spheroids: implications for tumor angiogenesis. Proc Natl Acad Sci USA 1995;92:768–72.
5. Kerbel R, Folkman J. Clinical translation of angiogenesis inhibitors. Nat Rev Cancer 2002;2:727–39.
6. Ferrara N, Davis-Smyth T. The biology of vascular endothelial growth factor. Endocr Rev 1997;18:4–25.
7. Rosen LS. Clinical experience with angiogenesis signaling inhibitors: focus on vascular endothelial growth factor (VEGF) blockers. Cancer Control 2002;9:36–44.
8. Kuo CJ, Farnebo F, Yu EY, et al. Comparative evaluation of the antitumor activity of antiangiogenic proteins delivered by gene transfer. Proc Natl Acad Sci USA 2001; 98:4605–10.
9. Cross MJ, Claesson-Welsh L. FGF and VEGF function in angiogenesis: signalling pathways, biological responses and therapeutic inhibition. Trends Pharmacol Sci 2001;22:201–7.
10. Autiero M, Luttun A, Tjwa M, Carmeliet P. Placental growth factor and its receptor, vascular endothelial growth factor receptor-1: novel targets for stimulation of ischemic tissue revascularization and inhibition of angiogenic and inflammatory disorders. J Thromb Haemostasis 2003;1:1356–70.
11. Veikkola T, Karkkainen M, Claesson-Welsh L, Alitalo K. Regulation of angiogenesis via vascular endothelial growth factor receptors. Cancer Res 2000;60:203–12.
12. Zachary I, Gliki G. Signaling transduction mechanisms mediating biological actions of the vascular endothelial growth factor family. Cardiovasc Res 2001;49:568–81.
13. Yu Y, Sato J. MAP kinases, phosphatidylinositol 3-kinase, and p70 S6 kinase mediate the mitogenic response of human endothelial cells to vascular endothelial growth factor. J Cell Physiol 1999;178:235–46.
14. Rousseau S, Houle F, Kotanides H, et al. Vascular endothelial growth factor (VEGF)-driven actin-based motility is mediated by VEGFR2 and requires concerted activation of stress-activated protein kinase 2 (SAPK2/p38) and geldanamycin-sensitive phosphorylation of focal adhesion kinase. J Biol Chem 2000;275:10661–72.
15. Gerber HP, McMurtrey A, Kowalski J, et al. Vascular endothelial growth factor regulates endothelial cell survival through the phosphatidylinositol 3′-kinase/Akt signal transduction pathway. Requirement for Flk-1/KDR activation. J Biol Chem 1998;273:30336–43.
16. Adlercreutz H. Western diet and Western diseases: some hormonal and biochemical mechanisms and associations. Scand J Clin Lab Investig Suppl 1990;201:3–23.
17. Miller AB. Diet and cancer. A review. Acta Oncol 1990;29:87–95.
18. Fotsis T, Pepper MS, Aktas E, et al. Flavonoids, dietary-derived inhibitors of cell proliferation and in vitro angiogenesis. Cancer Res 1997;57:2916–21.
19. Fotsis T, Pepper M, Adlercreutz H, et al. Genistein, a dietary ingested isoflavonoid, inhibits cell proliferation and in vitro angiogenesis. J Nutr 1995;125:790S–7S.
20. Papakonstanti EA, Stournaras C. Association of PI-3 kinase with PAK1 leads to actin phosphorylation and cytoskeletal reorganization. Mol Biol Cell 2002;13:2946–62.
21. Kroll J, Waltenberger J. The vascular endothelial growth factor receptor KDR activates multiple signal transduction pathways in porcine aortic endothelial cells. J Biol Chem 1997;272:32521–7.
22. Cooper JA, Hunter T. Changes in protein phosphorylation in Rous sarcoma virus-transformed chicken embryo cells. Mol Cell Biol 1981;1:165–78.
23. Ziche M, Morbidelli L, Choudhuri R, et al. Nitric oxide synthase lies downstream from vascular endothelial growth factor-induced but not basic fibroblast growth factor-induced angiogenesis. J Clin Investig 1997;99:2625–34.
24. Morbidelli L, Donnini S, Chillemi F, Giachetti A, Ziche M. Angiosuppressive and angiostimulatory effects exerted by synthetic partial sequences of endostatin. Clin Cancer Res 2003;9:5358–69.
25. Borsi L, Balza E, Carnemolla B, et al. Selective targeted delivery of TNFalpha to tumor blood vessels. Blood 2003;102:4384–92.
26. Pini A, Viti F, Santucci A, et al. Design and use of a phage display library. Human antibodies with subnanomolar affinity against a marker of angiogenesis eluted from a two-dimensional gel. J Biol Chem 1998;273:21769–76.
27. Scholzen T, Gerdes J. The Ki-67 protein: from the known and the unknown. J Cell Physiol 2000;182:311–22.
28. Parenti A, Morbidelli L, Cui XL, et al. Nitric oxide is an upstream signal of vascular endothelial growth factor-induced extracellular signal-regulated kinase1/2 activation in postcapillary endothelium. J Biol Chem 1998;273:4220–6.
29. Rousseau S, Houle F, Landry J, Huot J. p38 MAP kinase activation by vascular endothelial growth factor mediates actin reorganization and cell migration in human endothelial cells. Oncogene 1997;15:2169–77.
30. Gratton JP, Morales-Ruiz M, Kureishi Y, et al. Akt down-regulation of p38 signaling provides a novel mechanism of vascular endothelial growth factor-mediated cytoprotection in endothelial cells. J Biol Chem 2001;276:30359–65.

31. Burgering BM, Coffer PJ. Protein kinase B (c-Akt) in phosphatidylinositol-3-OH kinase signal transduction. Nature (Lond) 1995;376:599–602.
32. Franke T, Yang S, Chan T, et al. The protein kinase encoded by the Akt proto-oncogene is a target of the PDGF-activated phosphatidylinositol 3-kinase. Cell 1995;81:727–36.
33. Andjelkovic M, Alessi D, Meier R, et al. Role of translocation in the activation and function of protein kinase B. J Biol Chem 1997;272:31515–24.
34. Schmidt M, Fernandez de Mattos S, van der Horst A, et al. Cell cycle inhibition by FoxO forkhead transcription factors involves downregulation of cyclin D. Mol Cell Biol 2002;22:7842–52.
35. Diehl J, Cheng M, Roussel M, Sherr C. Glycogen synthase kinase-3beta regulates cyclin D1 proteolysis and subcellular localization. Genes Dev 1998;12:3499–511.
36. Weng Q, Kozlowski M, Belham C, et al. Regulation of the p70 S6 kinase by phosphorylation in vivo analysis using site-specific anti-phosphopeptide antibodies. J Biol Chem 1998;273:16621–9.
37. Joussen AM, Rohrschneider K, Reichling J, Kirchhof B, Kruse FE. Treatment of corneal neovascularization with dietary isoflavonoids and flavonoids. Exp Eye Res 2000;71:483–7.
38. Cao Y, Cao R. Angiogenesis inhibited by drinking tea. Nature (Lond) 1999;398:381.
39. Myoken Y, Kayada Y, Okamoto T, et al. Vascular endothelial cell growth factor (VEGF) produced by A-431 human epidermoid carcinoma cells and identification of VEGF membrane binding sites. Proc Natl Acad Sci USA 1991;88:5819–23.
40. Ueda H, Yamazaki C, Yamazaki M. Inhibitory effect of Perilla leaf extract and luteolin on mouse skin tumor promotion. Biol Pharm Bull 2003;26:560–3.
41. Graziani Y, Erikson E, Erikson RL. The effect of quercetin on the phosphorylation activity of the Rous sarcoma virus transforming gene product in vitro and in vivo. Eur J Biochem 1983;135:583–9.
42. Cunningham BD, Threadgill MD, Groundwater PW, Dale IL, Hickman JA. Synthesis and biological evaluation of a series of flavones designed as inhibitors of protein tyrosine kinases. Anticancer Drug Des 1992;7:365–84.
43. Datta SR, Brunet A, Greenberg ME. Cellular survival: a play in three Akts. Genes Dev 1999;13:2905–27.
44. Edinger A, Thompson C. Akt maintains cell size and survival by increasing mTOR-dependent nutrient uptake. Mol Biol Cell 2002;13:2276–88.
45. Madrid LV, Mayo MW, Reuther JY, Baldwin AS Jr. Akt stimulates the transactivation potential of the RelA/p65 subunit of NF-kappa B through utilization of the Ikappa B kinase and activation of the mitogen-activated protein kinase p38. J Biol Chem 2001;276:18934–40.
46. Opipari AW Jr, Hu HM, Yabkowitz R, Dixit VM. The A20 zinc finger protein protects cells from tumor necrosis factor cytotoxicity. J Biol Chem 1992;267:12424–7.
47. Yue T, Ni J, Romanic A, et al. TL1, a novel tumor necrosis factor-like cytokine, induces apoptosis in endothelial cells Involvement of activation of stress protein kinases (stress-activated protein kinase and p38 mitogen-activated protein kinase) and caspase-3-like protease. J Biol Chem 1999;274:1479–86.
48. Matsumoto T, Turesson I, Book M, Gerwins P, Claesson-Welsh L. p38 MAP kinase negatively regulates endothelial cell survival, proliferation, and differentiation in FGF-2-stimulated angiogenesis. J Cell Biol 2002;156:149–60.
49. Chan TO, Rittenhouse SE, Tsichlis PN. AKT/PKB and other D3 phosphoinositide-regulated kinases: kinase activation by phosphoinositide-dependent phosphorylation. Annu Rev Biochem 1999;68:965–1014.
50. Vanhaesebroeck B, Alessi DR. The PI3K-PDK1 connection: more than just a road to PKB. Biochem J 2000;346:561–76.
51. Walker EH, Pacold ME, Perisic O, et al. Structural determinants of phosphoinositide 3-kinase inhibition by wortmannin, LY294002, quercetin, myricetin, and staurosporine. Mol Cell 2000;6:909–19.
52. Thakker GD, Hajjar DP, Muller WA, Rosengart TK. The role of phosphatidylinositol 3-kinase in vascular endothelial growth factor signaling. J Biol Chem 1999;274:10002–7.
53. Abedi H, Zachary I. Vascular endothelial growth factor stimulates tyrosine phosphorylation and recruitment to new focal adhesions of focal adhesion kinase and paxillin in endothelial cells. J Biol Chem 1997;272:15442–51.
54. Jefferies HB, Fumagalli S, Dennis PB, et al. Rapamycin suppresses 5′TOP mRNA translation through inhibition of p70s6k. EMBO J 1997;16:3693–704.
55. Thomas G. An encore for ribosome biogenesis in the control of cell proliferation. Nat Cell Biol 2000;2:E71–2.
56. Chung J, Grammer TC, Lemon KP, Kazlauskas A, Blenis J. PDGF- and insulin-dependent pp70S6k activation mediated by phosphatidylinositol-3-OH kinase. Nature (Lond) 1994;370:71–5.
57. Reif K, Burgering BM, Cantrell DA. Phosphatidylinositol 3-kinase links the interleukin-2 receptor to protein kinase B and p70 S6 kinase. J Biol Chem 1997;272:14426–33.
58. Nave BT, Ouwens M, Withers DJ, Alessi DR, Shepherd PR. Mammalian target of rapamycin is a direct target for protein kinase B: identification of a convergence point for opposing effects of insulin and amino-acid deficiency on protein translation. Biochem J 1999;344:427–31.
59. Burnett PE, Barrow RK, Cohen NA, Snyder SH, Sabatini DM. RAFT1 phosphorylation of the translational regulators p70 S6 kinase and 4E-BP1. Proc Natl Acad Sci USA 1998;95:1432–7.
60. Chung J, Kuo CJ, Crabtree GR, Blenis J. Rapamycin-FKBP specifically blocks growth-dependent activation of and signaling by the 70 kd S6 protein kinases. Cell 1992;69:1227–36.
61. Dufner A, Andjelkovic M, Burgering BM, Hemmings BA, Thomas G. Protein kinase B localization and activation differentially affect S6 kinase 1 activity and eukaryotic translation initiation factor 4E-binding protein 1 phosphorylation. Mol Cell Biol 1999;19:4525–34.
62. Gonzalez-Garcia A, Garrido E, Hernandez C, et al. A new role for the p85-phosphatidylinositol 3-kinase regulatory subunit linking FRAP to p70 S6 kinase activation. J Biol Chem 2002;277:1500–8.
63. Peterson RT, Desai BN, Hardwick JS, Schreiber SL. Protein phosphatase 2A interacts with the 70-kDa S6 kinase and is activated by inhibition of FKBP12-rapamycin associated protein. Proc Natl Acad Sci USA 1999;96:4438–42.
64. Anderson K, Coadwell J, Stephens LR, Hawkins, P. Translocation of PDK-1 to the plasma membrane is important in allowing PDK-1 to activate protein kinase B. Curr Biol 1998;8:684–91.
65. Pullen N, Dennis P, Andjelkovic M, et al. Phosphorylation and activation of p70s6k by PDK1. Science (Wash DC) 1998;279:673–4.
66. Romanelli A, Dreisbach V, Blenis J. Characterization of phosphatidylinositol 3-kinase-dependent phosphorylation of the hydrophobic motif site Thr^{389} in p70 S6 kinase 1. J Biol Chem 2002;277:40281–9.
67. Wu L, Mayo L, Dunbar J, et al. Utilization of distinct signaling pathways by receptors for vascular endothelial cell growth factor and other mitogens in the induction of endothelial cell proliferation. J Biol Chem 2000;275:5096–103.
68. Kuhnau, J. The flavonoids A class of semi-essential food components: their role in human nutrition. World Rev Nutr Diet 1976;24:117–91.
69. Scalbert A, Williamson G. Dietary intake and bioavailability of polyphenols. J Nutr 2000;130:2073S–85S.
70. Adlercreutz H, van der Wildt J, Kinzel J, et al. Lignan and isoflavonoid conjugates in human urine. J Steroid Biochem Mol Biol 1995;52:97–103.
71. Erlund I, Meririnne E, Alfthan G, Aro A. Plasma kinetics and urinary excretion of the flavanones naringenin and hesperetin in humans after ingestion of orange juice and grapefruit juice. J Nutr 2001;131:235–41.
72. Maiani G, Serafini M, Salucci M, Azzini E, Ferro-Luzzi A. Application of a new high-performance liquid chromatographic method for measuring selected polyphenols in human plasma. J Chromatogr B Biomed Sci Appl 1997;692:311–7.
73. Manach C, Morand C, Demigne C, et al. Bioavailability of rutin and quercetin in rats. FEBS Lett 1997;409:12–6.

Luteolin Inhibits Vascular Endothelial Growth Factor-Induced Angiogenesis; Inhibition of Endothelial Cell Survival and Proliferation by Targeting Phosphatidylinositol 3′-Kinase Activity

Eleni Bagli, Maria Stefaniotou, Lucia Morbidelli, et al.

Cancer Res 2004;64:7936-7946.